

**Planar Quadrotor:**  
**Extended Kalman Filter Design**

Arseni Lysak, Tsimafei Iliusenka, John Elvin Ndahiro, Pablo Calderon Mateo

Aeronautical Systems Integration

January 19, 2026

## Contents

Introduction	2
System modeling	2
Quadcopter Definition	4
Clean Simulation	6
Real-World Trajectory	7
Extended Kalman Filter Design	8
Jacobian for Covariance Propagation . . . . .	9
Prediction Step . . . . .	11
Correction Step . . . . .	11
Running Mean Filter	13
Results & Visualization	15
Analysis of Estimation Performance . . . . .	31
Robustness Testing Methodology . . . . .	32
Robustness Analysis Conclusions . . . . .	33
Team Member Contributions	34
Formal Roles . . . . .	34
Actual Tasks . . . . .	34
Planar_Quadrotor.m	37
simulation_quadrotor.m	41
robustness.m	50

## Introduction

The aim of this project is to implement an Extended Kalman Filter (EKF) to estimate the movement of a 2D planar quadrotor (fig. 1) utilizing noisy sensor measurements.

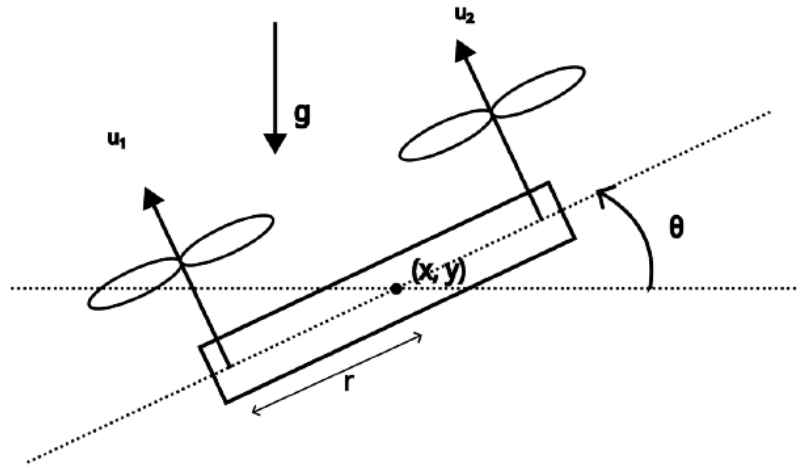


Figure 1: Diagram of the Planar Quadrotor System.

## System modeling

The movement of the quadrotor is governed by the following nonlinear equations of motion:

$$m\ddot{x} = -(u_1 + u_2) \sin \theta \quad (1)$$

$$m\ddot{y} = (u_1 + u_2) \cos \theta - mg \quad (2)$$

$$I\ddot{\theta} = r(u_1 - u_2) \quad (3)$$

where:

- $m$ : mass of the quadrotor

- $I$ : moment of inertia
- $r$ : distance from the center of mass to the rotors
- $g$ : gravitational acceleration
- $u_1, u_2$ : rotor thrust forces

This would imply that the system state is represented by a six-element vector  $\mathbf{x}$ , and the control input is represented by a two-element vector  $\mathbf{u}$ :

$$\mathbf{x} = \begin{bmatrix} x \\ \dot{x} \\ y \\ \dot{y} \\ \theta \\ \dot{\theta} \end{bmatrix}, \quad \mathbf{u} = \begin{bmatrix} u_1 \\ u_2 \end{bmatrix} \quad (4)$$

To complete the system model, the observation vector  $\mathbf{z}$  is defined based on the onboard sensors. It is important to note that while a real-world **Inertial Measurement Unit (IMU)** measures linear acceleration and angular velocity—requiring fusion algorithms to estimate orientation—this simulation adopts a simplification where the IMU directly provides the pitch angle ( $\theta$ ) and pitch rate ( $\dot{\theta}$ ). Combined with an **altimeter** that measures vertical position ( $y$ ), the observation model becomes a linear mapping of the state vector:

$$\mathbf{z} = C\mathbf{x} = \begin{bmatrix} 0 & 0 & 1 & 0 & 0 & 0 \\ 0 & 0 & 0 & 0 & 1 & 0 \\ 0 & 0 & 0 & 0 & 0 & 1 \end{bmatrix} \begin{bmatrix} x \\ \dot{x} \\ y \\ \dot{y} \\ \theta \\ \dot{\theta} \end{bmatrix} = \begin{bmatrix} y \\ \theta \\ \dot{\theta} \end{bmatrix} \quad (5)$$

### Quadcopter Definition

The quadrotor system parameters were initialized with a mass  $m = 0.5$  kg, a rotor arm length  $r = 0.15$  m, and a moment of inertia  $I = 0.005$  kg · m<sup>2</sup>. The simulation utilizes a time step of  $dt = 0.01$  s under standard gravitational acceleration  $g = 9.81$  m/s<sup>2</sup>. Baseline rotor thrust forces are  $u_1 = 5$  N and  $u_2 = 5$  N (Appendix A, lines 8-15).

Four scenarios for control inputs were chosen (Appendix A, lines 53-96):

1. Flying up. For the simplest case, both rotors are set to 3 N (fig. 3).
2. Recovery from horizontal flight (fig. 4). To do this, the quadrotor system must rotate to have significant vertical thrust component. Three control stages are:
  - a) Initiate rotation. For 1.1 s create rotational moment by 0.05 N thrust difference between the rotors (4.05 N, 4.0 N).
  - b) Stop the rotation. For the next 1.1 s we slow down the rotation with the opposing thrust moment (4.0 N, 4.05 N).
  - c) Increase altitude. For the rest of the simulation time we pull up with same thrust of 4 N on both rotors.

3. 360 degree roll (fig. 5). This is the most complicated control-wise, due to the choice of long rotation. Altitude loss is significant. Four control stages are:

- a) Initiate rotation. A small thrust difference is applied for the first 2 seconds (4.04 N, 4 N).
  - b) Let it rotate. For a second, the system is set to 0 thrust to let it rotate freely.
  - c) Stop the rotation. For another 2 seconds, we slow down the rotation, only using small thrust to avoid increasing falling speed (0 N, 0.04 N).
  - d) Recover lost altitude. After 5 seconds of accurate controls, we set both rotors to their maximum (5 N) to avoid collision with the ground.
4. Straight fall recovery (fig. 6). Almost identical to the first case, however slightly higher thrust is assumed (3.2 N on both rotors).

The small thrust variation of the rotor is inherently periodic and is recreated using simple trigonometric functions (cosine for rotor  $u_1$ , sine for rotor  $u_2$ ).

Moreover, a unique set of initial conditions was defined for each case (Appendix A, lines 99-102):

1. Zero velocity in both directions, system is 1 m above the ground, no rotation.
2. The system is assumed to have a horizontal speed of 3 m/s at 10 m altitude, rotors' thrust is parallel to the ground.
3. High vertical speed and altitude (5 m/s and 50 m respectively) are assumed. No initial rotational speed, system tilt or horizontal speed.

4. Negative horizontal and vertical velocities (-1 m/s and -3 m/s respectively), altitude of 15 m. Quadrotor system is initially tilted down by around 18 degrees to align rotor thrust direction with total velocity vector.

### Clean Simulation

Equations 1-3 represent perfect conditions as they do not account for process noise. The state vector for this ideal trajectory is designated as `state.clean` in the code (Appendix B, line 24). This ensures the prediction adheres to the actual physical dynamics.

The clean simulation utilizes first-order Euler integration to propagate the system state forward in time. At each time step  $t$ , the state increments are computed based on the previous state vector  $\mathbf{x}_{t-1}$  and the current control inputs (Appendix B, lines 60-71). The positional and angular updates are derived linearly from the previous velocities:

$$\Delta x = \dot{x}_{t-1} \Delta t, \quad \Delta y = \dot{y}_{t-1} \Delta t, \quad \Delta \theta = \dot{\theta}_{t-1} \Delta t \quad (6)$$

The changes in linear and angular velocities are calculated by discretizing the dynamic equations of motion (Eq.1-3). These updates account for the non-linear coupling introduced by the quadrotor's orientation  $\theta$ :

$$\Delta \dot{x} = -\frac{(u_1 + u_2)}{m} \sin(\theta_{t-1}) \Delta t \quad (7)$$

$$\Delta \dot{y} = \left( \frac{(u_1 + u_2)}{m} \cos(\theta_{t-1}) - g \right) \Delta t \quad (8)$$

$$\Delta \dot{\theta} = \frac{r}{I} (u_1 - u_2) \Delta t \quad (9)$$

Finally, the state vector is updated by adding these increments to the previous state,  $\mathbf{x}_t = \mathbf{x}_{t-1} + \Delta\mathbf{x}$ , and the ideal sensor output is computed as  $\mathbf{y}_t = C\mathbf{x}_t$  (Appendix B, lines 75, 76).

### Real-World Trajectory

The real-world trajectory (`state.real`) differs from the perfect trajectory solely through the introduction of process and measurement noise. It is assumed that both process and measurement noise follow a **Gaussian** distribution, which is implemented in the simulation using the MATLAB function `randn` (Appendix B, lines 95-96). The stochastic properties are defined by their variances: the process noise variance is set to  $0.003^2$ , while the measurement noise variance is set to  $0.01^2$  (Appendix B, lines 47-50).

The governing equations 1-3 remain unchanged, with noise injected during the state update step. The true state evolution is modeled by adding a stochastic process noise vector  $\mathbf{w}$  to the deterministic dynamics:

$$\mathbf{x}_t = \mathbf{x}_{t-1} + \Delta\mathbf{x} + \mathbf{w}_{t-1} \quad (10)$$

Subsequently, the simulated sensor measurements  $\mathbf{z}_t$  are generated by applying the measurement matrix  $C$  to the updated state, with the addition of measurement noise  $\mathbf{v}_t$ :

$$\mathbf{z}_t = C\mathbf{x}_t + \mathbf{v}_t \quad (11)$$

## Extended Kalman Filter Design

The Linear Kalman filter addresses the general problem of trying to estimate the state of a discrete-time controlled process that is governed by a linear stochastic difference equation. A Kalman filter that linearizes about the current mean and covariance is referred to as an extended Kalman filter or EKF.

The EKF is employed because the quadrotor system is nonlinear—motion is dependent on the sine and cosine of the angle  $\theta$ . The EKF linearizes the system at each time step using the current optimal estimate prior to applying standard Kalman update equations.

The working principle of the filter is optimally weighting sensor measurements against the predicted values in accordance with the ideal mathematical model (fig. 2).

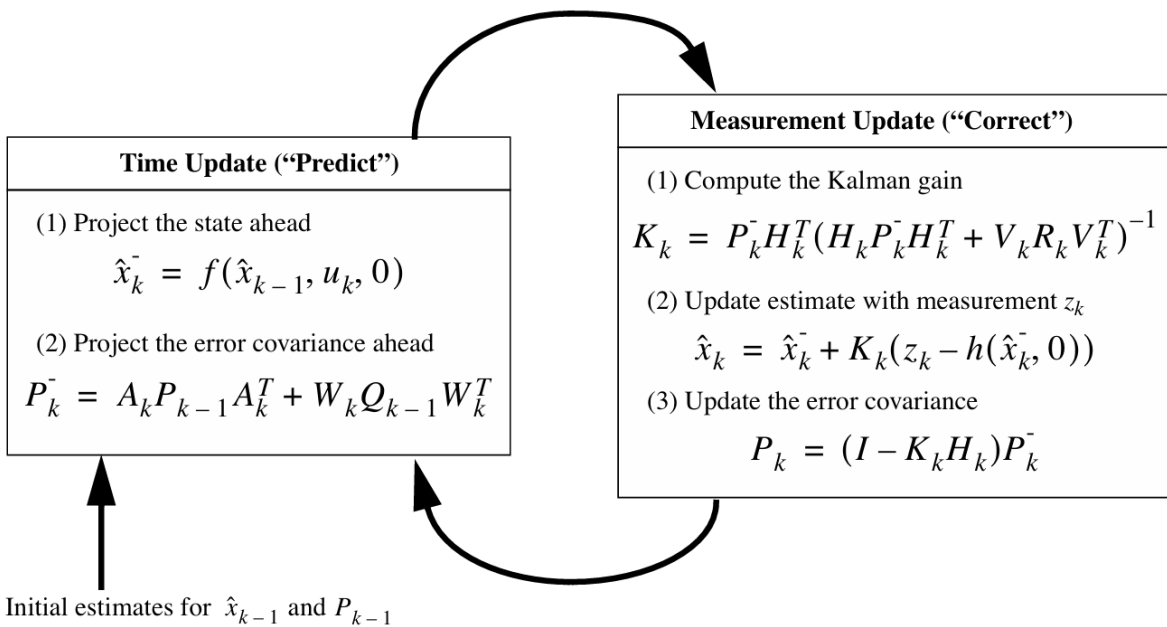


Figure 2: A complete picture of the operation of the extended Kalman filter. Source: Greg Welch and Gary Bishop, *An Introduction to the Kalman Filter*, Technical Report TR 95-041, Updated March 11, 2002 (University of North Carolina at Chapel Hill, 2002).

### Jacobian for Covariance Propagation

To estimate a process with non-linear difference and measurement relationships, the system is modeled using non-linear functions  $f$  and  $h$ :<sup>1</sup>

$$\mathbf{x}_{k+1} = f(\mathbf{x}_k, \mathbf{u}_k) + \mathbf{w}_k \quad (12)$$

$$\mathbf{z}_k = h(\mathbf{x}_k) + \mathbf{v}_k \quad (13)$$

where:

- $\mathbf{x}_k$  is the state vector at time step  $k$ ,
- $\mathbf{z}_k$  is the measurement vector,
- $\mathbf{u}_k$  is the control input vector,
- $\mathbf{w}_k$  and  $\mathbf{v}_k$  are the process and measurement noise vectors respectively.

To linearize the estimate for covariance propagation, the Jacobian matrices  $\mathbf{F}$  and  $\mathbf{H}$  have to be computed:

- $\mathbf{F}_k$  is the Jacobian of the dynamics function  $f$  with respect to the state  $\mathbf{x}$ , evaluated at the previous estimate  $\hat{\mathbf{x}}_{k-1|k-1}$  :  $[\mathbf{F}_k = \frac{\partial f}{\partial \mathbf{x}} \Big| \hat{\mathbf{x}}_{k-1|k-1}, \mathbf{u}_k]$
- $\mathbf{H}_k$  is the Jacobian of the measurement function  $h$  with respect to the state  $\mathbf{x}$ , evaluated at the predicted state  $\hat{\mathbf{x}}_{k|k-1}$  :  $[\mathbf{H}_k = \frac{\partial h}{\partial \mathbf{x}} \Big| \hat{\mathbf{x}}_{k|k-1}]$

---

1. Greg Welch and Gary Bishop, *An Introduction to the Kalman Filter*, Technical Report TR 95-041, Updated March 11, 2002 (University of North Carolina at Chapel Hill, 2002).

To update the error covariance, the state transition Jacobian  $A$  is derived from the partial derivatives of the dynamics, which are defined by equations 1 - 3:

$$\frac{\partial \ddot{x}}{\partial \theta} = -\frac{\cos \theta}{m}(u_1 + u_2) \quad (14)$$

$$\frac{\partial \ddot{y}}{\partial \theta} = -\frac{\sin \theta}{m}(u_1 + u_2) \quad (15)$$

The resulting Jacobian  $A$  is (Appendix A, lines 30-35):

$$A = \begin{bmatrix} 0 & 1 & 0 & 0 & 0 & 0 \\ 0 & 0 & 0 & 0 & \frac{-\cos(\theta)(u_1+u_2)}{m} & 0 \\ 0 & 0 & 0 & 1 & 0 & 0 \\ 0 & 0 & 0 & 0 & \frac{-\sin(\theta)(u_1+u_2)}{m} & 0 \\ 0 & 0 & 0 & 0 & 0 & 1 \\ 0 & 0 & 0 & 0 & 0 & 0 \end{bmatrix} \quad (16)$$

The discrete-time state transition matrix  $F$  used in the EKF is defined as  $F = I + A\Delta t$ , where  $I$  represents the identity matrix and  $A\Delta t$  represents the change over the time step.

$$F = \begin{bmatrix} 1 & \Delta t & 0 & 0 & 0 & 0 \\ 0 & 1 & 0 & 0 & \frac{-\cos(\theta)(u_1+u_2)}{m}\Delta t & 0 \\ 0 & 0 & 1 & \Delta t & 0 & 0 \\ 0 & 0 & 0 & 1 & \frac{-\sin(\theta)(u_1+u_2)}{m}\Delta t & 0 \\ 0 & 0 & 0 & 0 & 1 & \Delta t \\ 0 & 0 & 0 & 0 & 0 & 1 \end{bmatrix} \quad (17)$$

The measurement matrix  $H$  (referred to as  $C$  in code) (Appendix A, lines 41-43) is defined as:

$$H = C = \begin{bmatrix} 0 & 0 & 1 & 0 & 0 & 0 \\ 0 & 0 & 0 & 0 & 1 & 0 \\ 0 & 0 & 0 & 0 & 0 & 1 \end{bmatrix} \quad (18)$$

The implementation follows a standard **predict–correct cycle** (fig. 2), executing in real-time within the simulation loop.

#### Prediction Step

First, the states are updated, and the estimate is stored as `state.estimate`.

Following the state acquisition for the current timestep, the  $F$  matrix is updated based on the current angle (`theta_estimate`) and thrust (`control_input`). This dependency characterizes the Extended Kalman Filter. The error covariance is then predicted:

$$P_k^- = A_k P_{k-1} A_k^T + Q_{k-1} \quad (19)$$

where  $Q$  represents the confidence in the physics model.

#### Correction Step

The estimate is subsequently corrected using the latest noisy sensor data (`output.real`). The measurement residual—the discrepancy between sensor readings and predictions—is computed:

The measurement residual, also known as the innovation, quantifies the discrepancy between the actual sensor measurements and the predicted output based on the a priori

state estimate. It is computed as:

$$\tilde{\mathbf{y}}_k = \mathbf{z}_k - C\hat{\mathbf{x}}_k^- \quad (20)$$

where  $\mathbf{z}_k$  represents the noisy sensor measurement vector at time step  $k$ , and  $C\hat{\mathbf{x}}_k^-$

represents the predicted measurement derived from the current state estimate.

The Kalman gain  $K$  is calculated to determine the weighting between sensor data and physics predictions:

$$S = CP_k^- C^T + R \quad (21)$$

$$K = P_k^- C^T S^{-1} \quad (22)$$

The process noise covariance  $Q$  and measurement noise covariance  $R$  were defined as

$I \times 0.003^2$  and  $I \times 0.01^2$ , respectively. This effectively means that the filter is "perfectly tuned."

Finally, the state and covariance matrices are updated to obtain the posteriori estimates. The state estimate is corrected by adding the measurement residual, weighted by the Kalman gain  $K$  (Appendix B, lines 145-146):

$$\hat{\mathbf{x}}_k = \hat{\mathbf{x}}_k^- + K_k \tilde{\mathbf{y}}_k \quad (23)$$

Subsequently, the error covariance matrix  $P$  is updated to reflect the reduced uncertainty following the incorporation of the measurement:

$$P_k = (I - K_k C) P_k^- \quad (24)$$

### Running Mean Filter

In order to compare the performance of the EKF, the running mean filter was implemented. With a window size of 10 (Appendix B, line 53), it simply averages the values from the last 10 time steps when processing sensor measurements. It then uses this data to predict the change in states.

The running mean filter implementation employs a hybrid estimation strategy. First, a sliding window average is applied to the noisy sensor measurements to attenuate high-frequency jitters. For a window size  $N$ , the smoothed measurement vector  $\bar{\mathbf{z}}_t$  is computed as the arithmetic mean of the past  $N$  observations (Appendix B, lines 162-164):

$$\bar{\mathbf{z}}_t = \frac{1}{N} \sum_{k=t-N+1}^t \mathbf{z}_k \quad (25)$$

These smoothed measurements are directly substituted into the state vector for the observable variables ( $y$ ,  $\theta$ , and  $\dot{\theta}$ ), bypassing the dynamic model for these specific degrees of freedom. For the remaining unobserved states ( $x$ ,  $\dot{x}$ , and  $\dot{y}$ ), the filter utilizes the system dynamics (Eq. 1-2) for propagation. Crucially, these dynamic updates rely on the smoothed orientation angle  $\theta_t$  rather than the previous state estimate. The horizontal position is updated kinematically, while the velocity increments are derived from the thrust

projections:

$$\Delta x = \dot{x}_{t-1} \Delta t \quad (26)$$

$$\Delta \dot{x} = -\frac{(u_1 + u_2)}{m} \sin(\theta_t) \Delta t \quad (27)$$

$$\Delta \dot{y} = \left( \frac{(u_1 + u_2)}{m} \cos(\theta_t) - g \right) \Delta t \quad (28)$$

Finally, these computed increments are applied to update the estimates for the horizontal position and linear velocities (Appendix B, lines 169–175).

## Results & Visualization

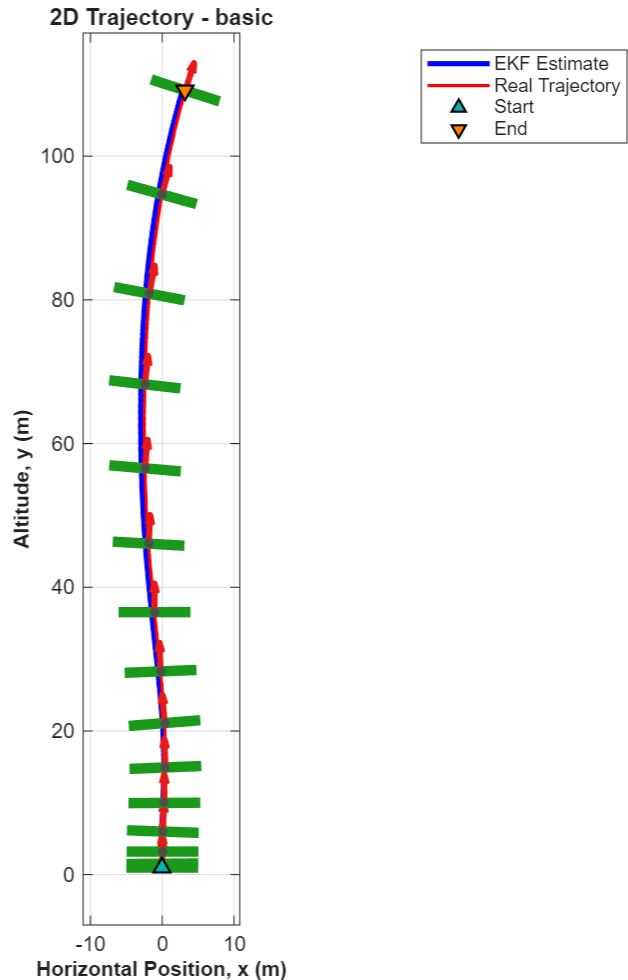


Figure 3: 2D trajectory for the basic hover scenario, comparing EKF estimate against the real noisy path.

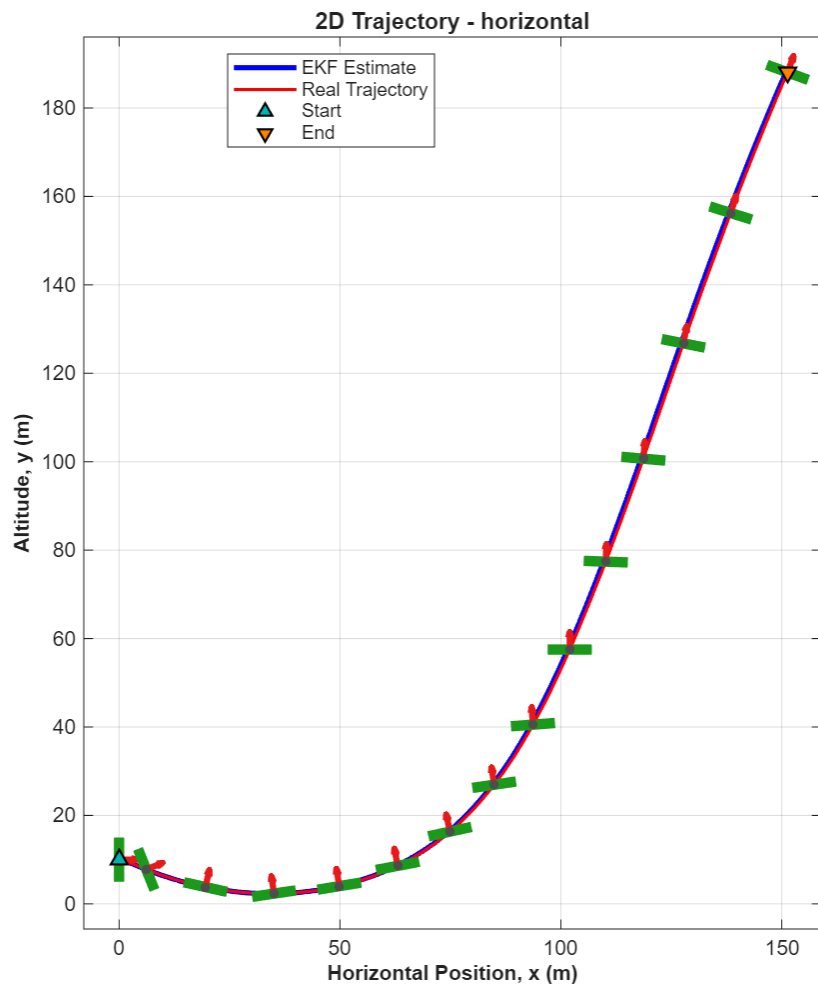


Figure 4: 2D trajectory for the horizontal recovery scenario, showing EKF performance during lateral motion.

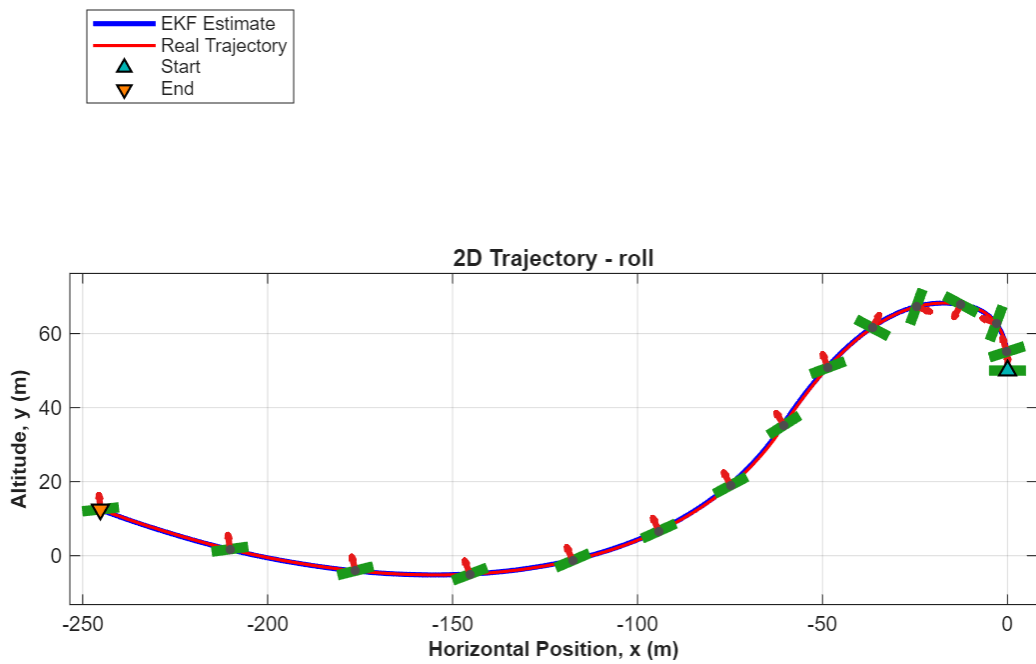


Figure 5: 2D trajectory for the  $360^\circ$  roll scenario, illustrating EKF tracking during aggressive rotational motion.

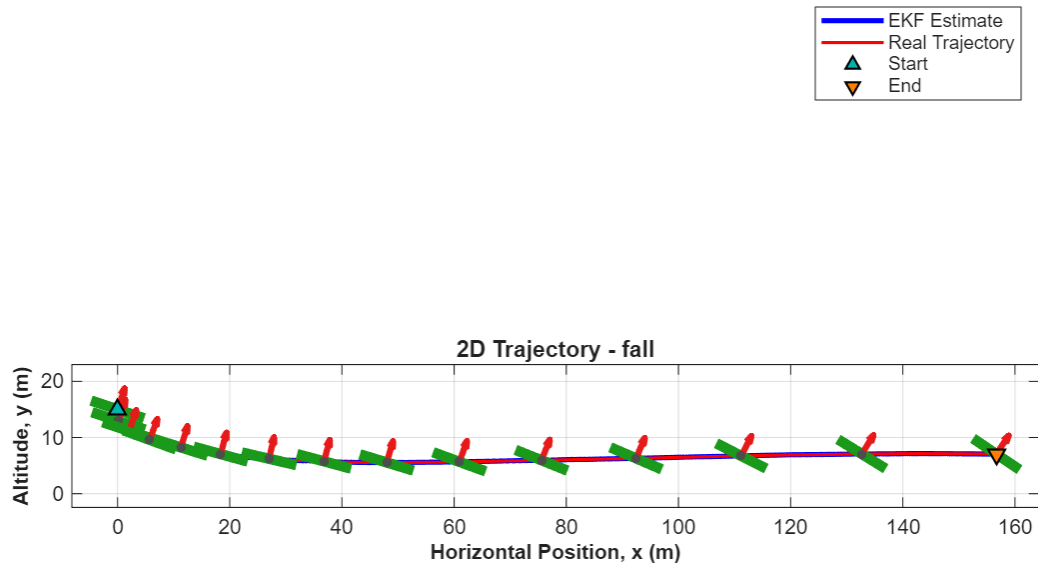


Figure 6: 2D trajectory for the straight fall recovery scenario, demonstrating EKF accuracy during descent.

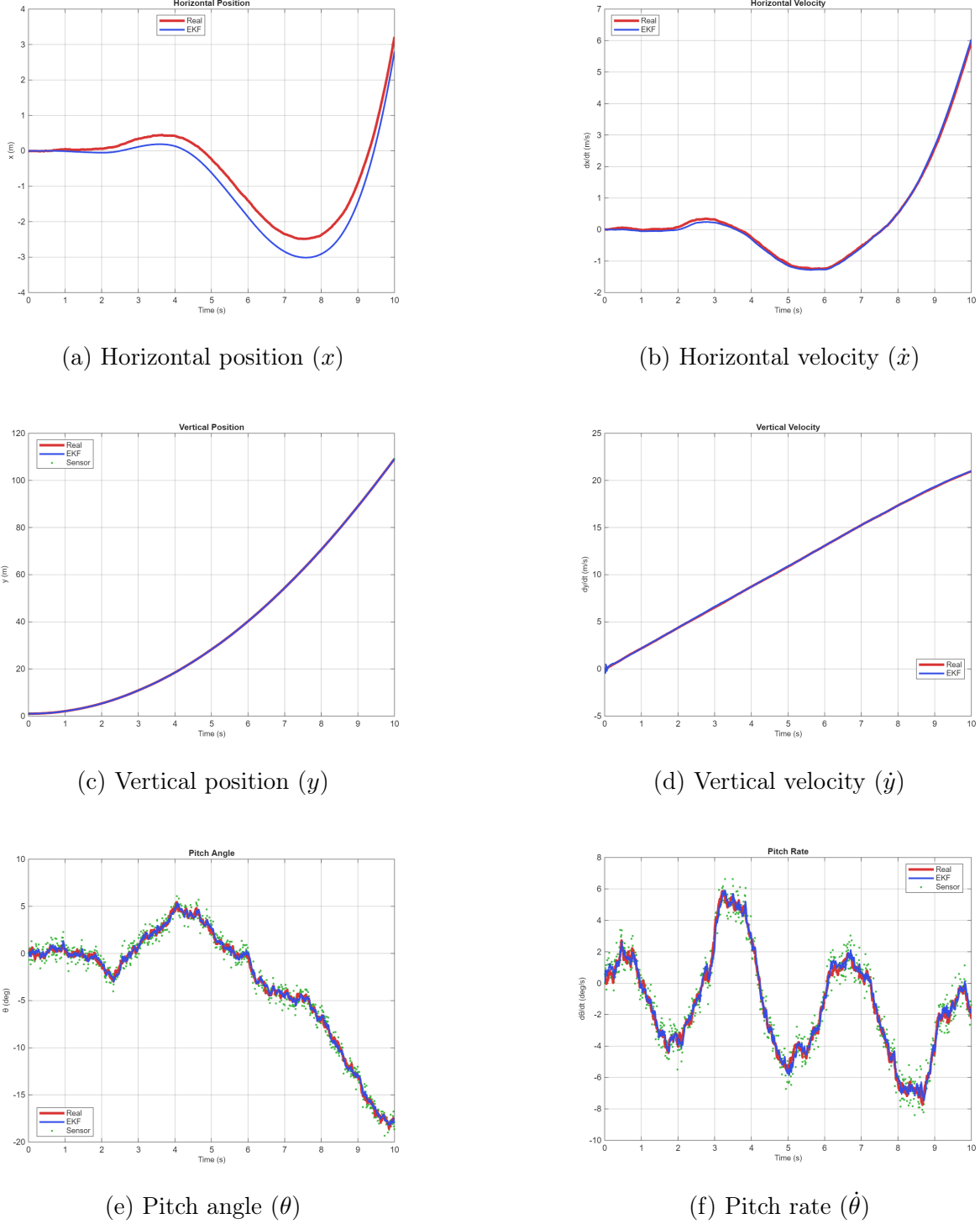


Figure 7: State variables over time for the basic scenario. (a): Horizontal position ( $x$ ): a small lateral displacement is caused by slight thrust asymmetry that induces a small rotation of the vehicle. (b): Horizontal velocity ( $\dot{x}$ ): oscillates around zero, indicating minor alternating horizontal accelerations. (c): Vertical position ( $y$ ): shows continuous ascent with no reversal in direction. (d): Vertical velocity ( $\dot{y}$ ): remains positive and increases smoothly, confirming upward motion. (e): Pitch angle ( $\theta$ ): positive and negative values represent alternating nose-up and nose-down orientations. (f): Pitch rate ( $\dot{\theta}$ ): zero crossings correspond to changes in rotational direction.

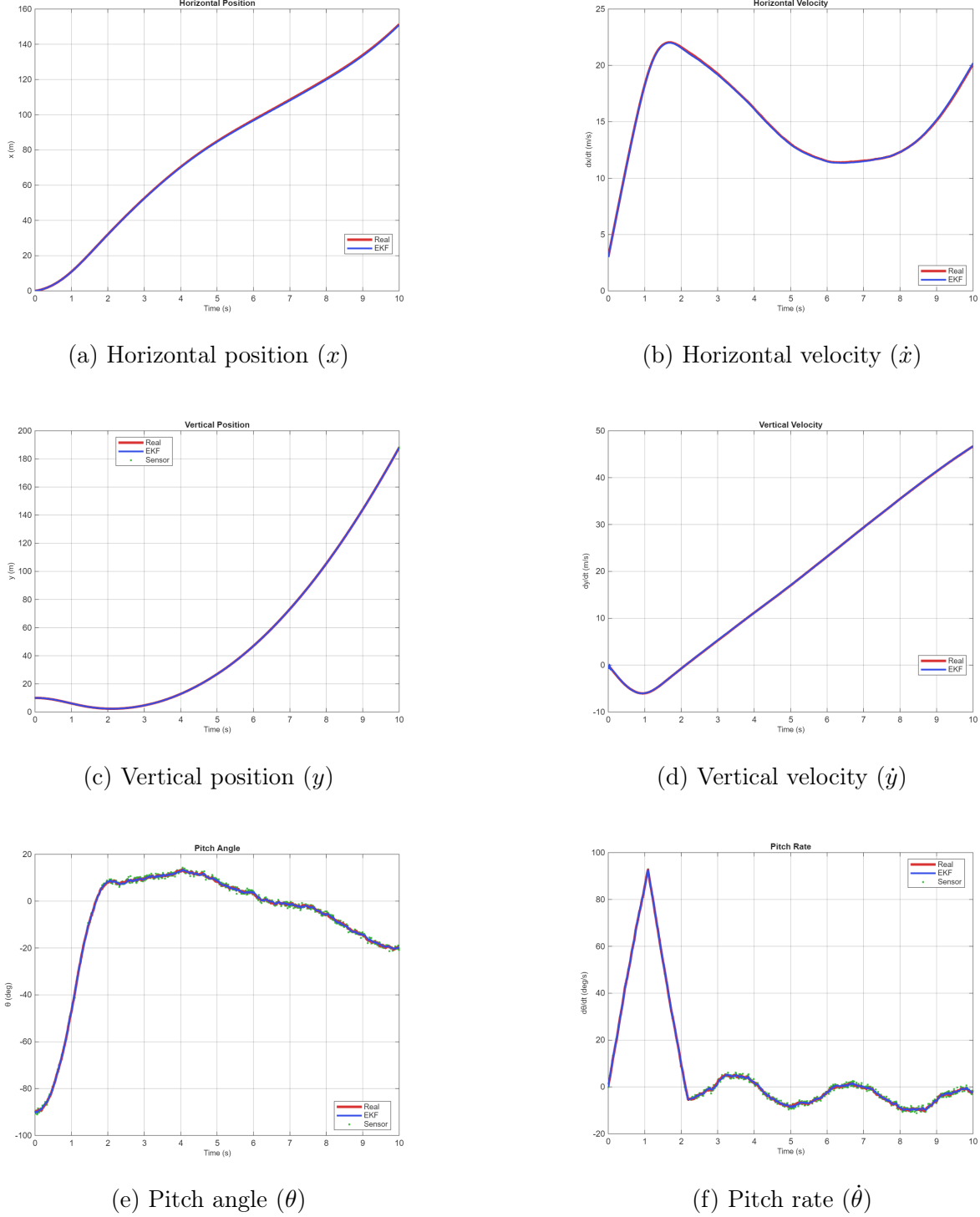


Figure 8: State variables over time for the horizontal and horizontal recovery scenarios. (a) Horizontal position ( $x$ ): shows sustained lateral movement in a single direction. (b) Horizontal velocity ( $\dot{x}$ ): variations in slope indicate acceleration and deceleration phases. (c) Vertical position ( $y$ ): decreases initially then increases. (d) Vertical velocity ( $\dot{y}$ ): negative values indicate descent and the zero crossing marks direction reversal. (e) Pitch angle ( $\theta$ ): shows rapid attitude change followed by gradual stabilization. (f) Pitch rate ( $\dot{\theta}$ ): is characterized by high initial rotation rates that later reduce in magnitude.

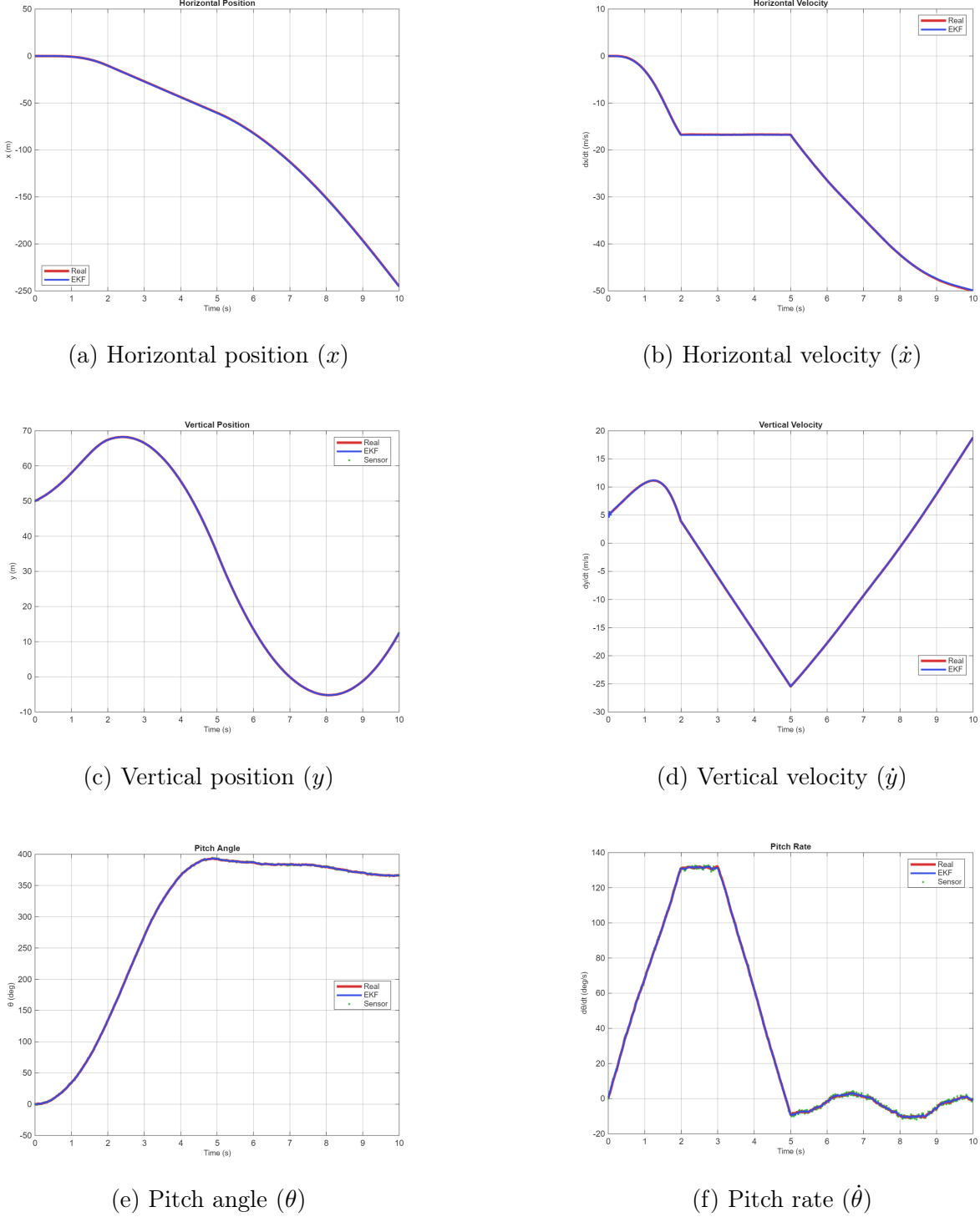


Figure 9: State variables over time for the roll scenario. (a) Horizontal position ( $x$ ): decreases continuously, indicating motion opposite to the reference direction. (b) Horizontal velocity ( $\dot{x}$ ): remains negative throughout, confirming persistent backward motion. (c) Vertical position ( $y$ ): shows alternating ascent and descent with clear extrema. (d) Vertical velocity ( $\dot{y}$ ): exhibits multiple zero crossings, indicating repeated reversals in vertical motion. (e) Pitch angle ( $\theta$ ): exceeds  $360^\circ$ , confirming completion of a full rotational maneuver. (f) Pitch rate ( $\dot{\theta}$ ): shows large positive values indicating rapid rotation and negative values marking deceleration.

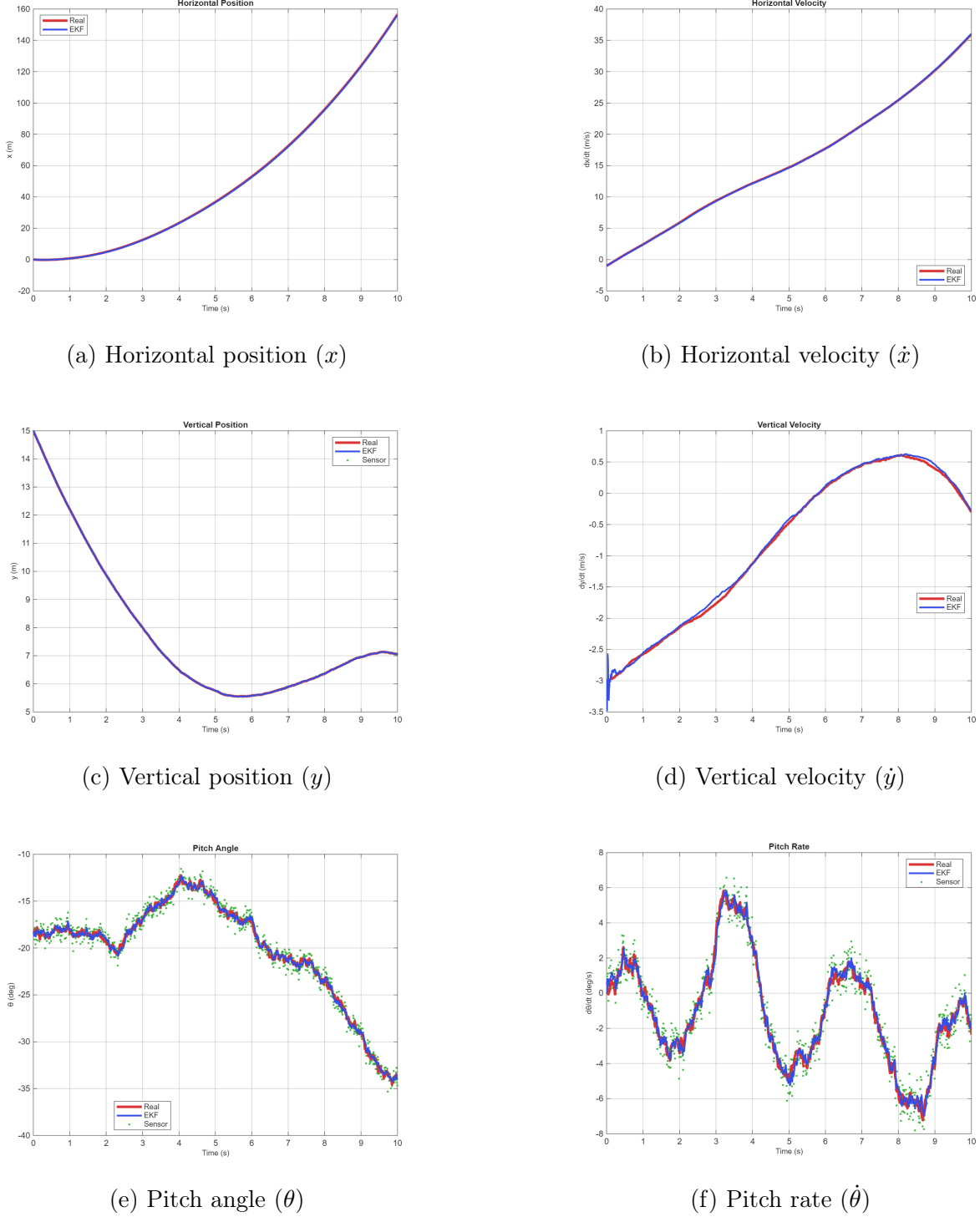


Figure 10: State variables over time for the fall scenario. (a) Horizontal position ( $x$ ): shows continuous forward motion during descent. (b) Horizontal velocity ( $\dot{x}$ ): increases almost linearly, indicating constant horizontal acceleration. (c) Vertical position ( $y$ ): decreases to a minimum before slight recovery, marking the lowest altitude reached. (d) Vertical velocity ( $\dot{y}$ ): is negative during free fall and approaching zero as recovery thrust is applied. (e) Pitch angle ( $\theta$ ): shows progressive nose-down rotation caused by loss of vertical stability. (f) Pitch rate ( $\dot{\theta}$ ): oscillates with sign changes that reflect alternating rotational actions due to the process noise.

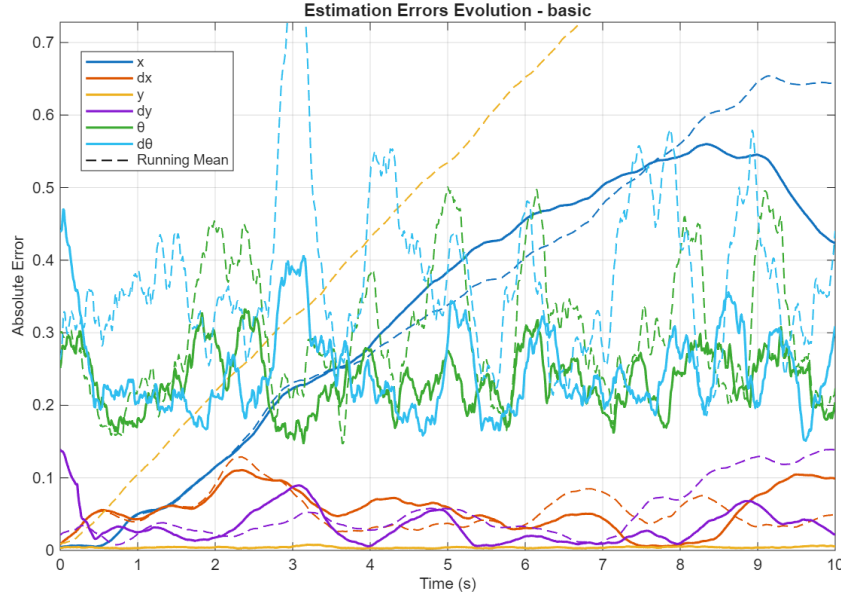


Figure 11: Absolute estimation errors for all states over time (basic scenario), comparing EKF and running mean filters. While some states show varying benefit of EKF over running mean ( $x, \dot{x}, \dot{y}$ ), and others show significant error spikes of running mean ( $\theta, \dot{\theta}$ ),  $y$  in particular displays constant growth of running mean error, while its EKF error stays almost constant.

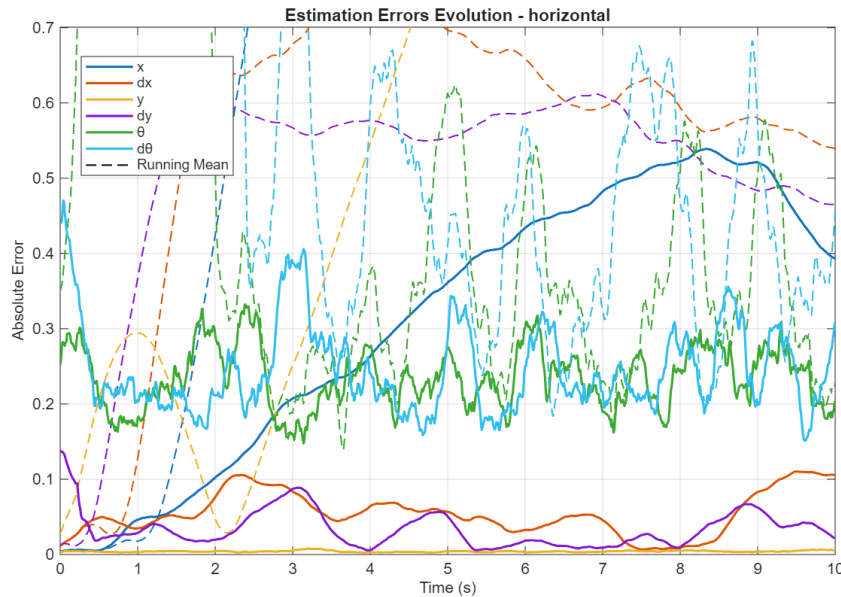


Figure 12: Absolute estimation errors for all states over time (horizontal recovery scenario). With a more control-heavy case, running mean errors show significant increase, unbound in cases of  $x$ ,  $y$  and  $\theta$ .

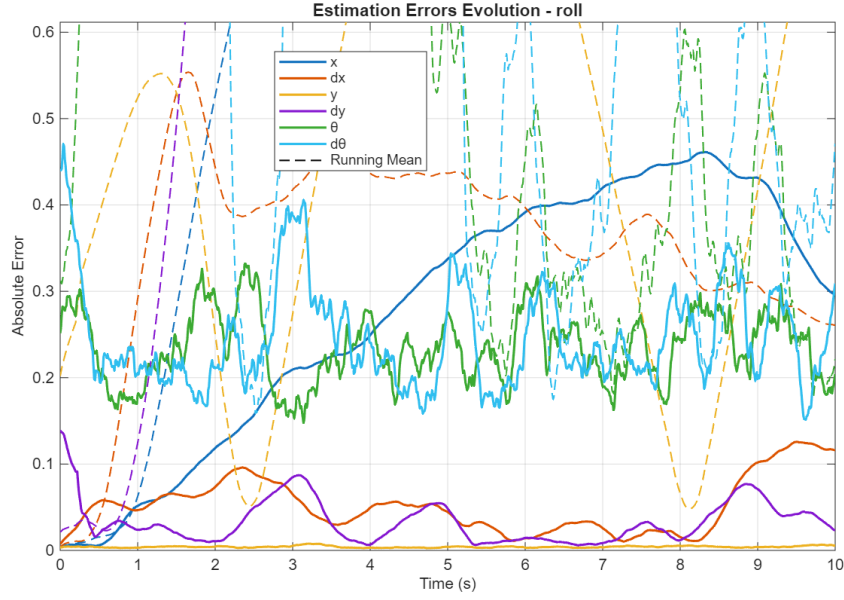


Figure 13: Absolute estimation errors for all states over time (roll scenario). This challenging simulation shows unreliability of running mean for complicated system movement.

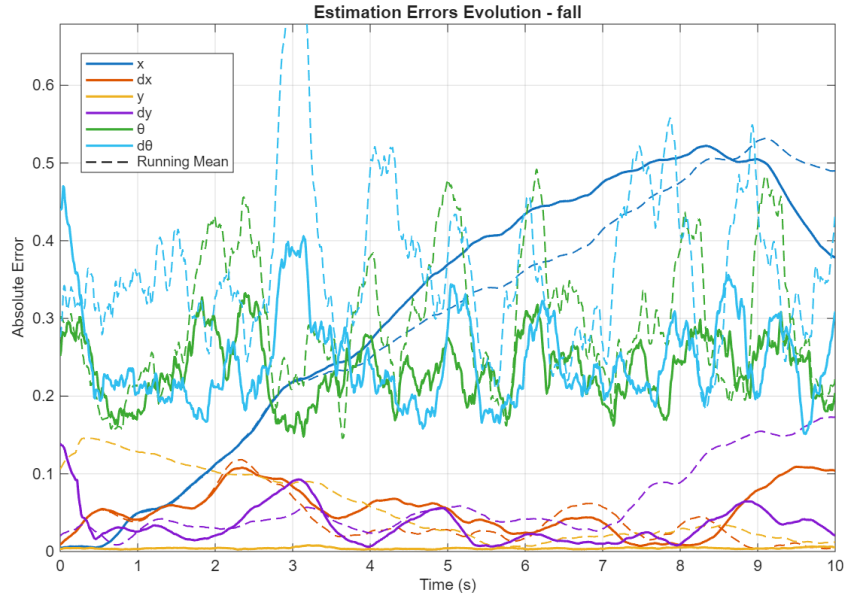


Figure 14: Absolute estimation errors for all states over time (fall recovery scenario). Not explicitly rotating system, just like the basic scenario, shows varying accuracy of running mean. Although  $y$  error is now bounded, error spikes of  $\theta$  and  $\dot{\theta}$  cannot be ignored.

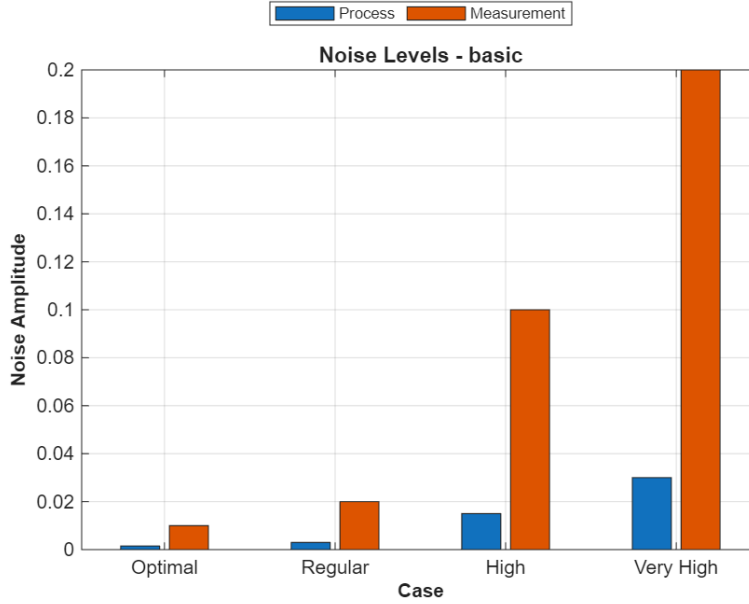


Figure 15: Process and measurement variance for robustness analysis. These values don't vary between the scenarios.

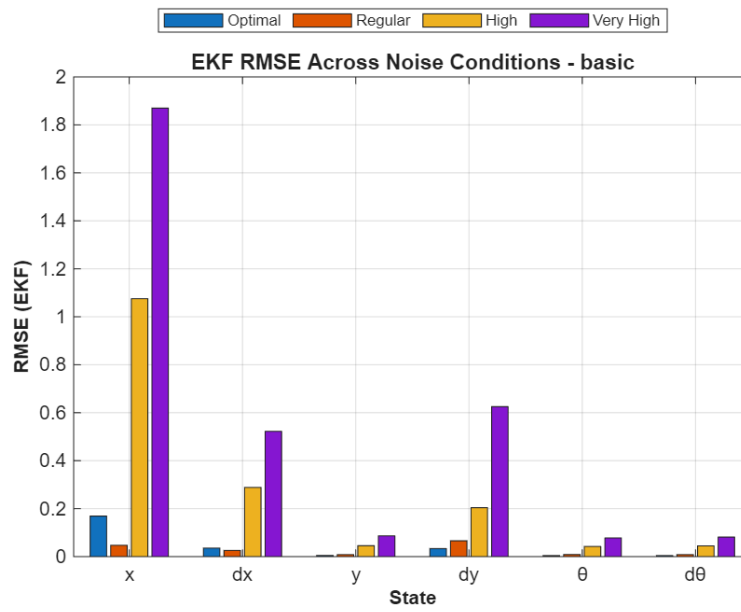


Figure 16: EKF RMSE across four noise levels for each state (basic scenario). For the most part, RMSE increases along with variance, however  $x$  and  $\dot{x}$  are slightly different due to their progressing Euler integration error. Same trend can be expected in the other cases.

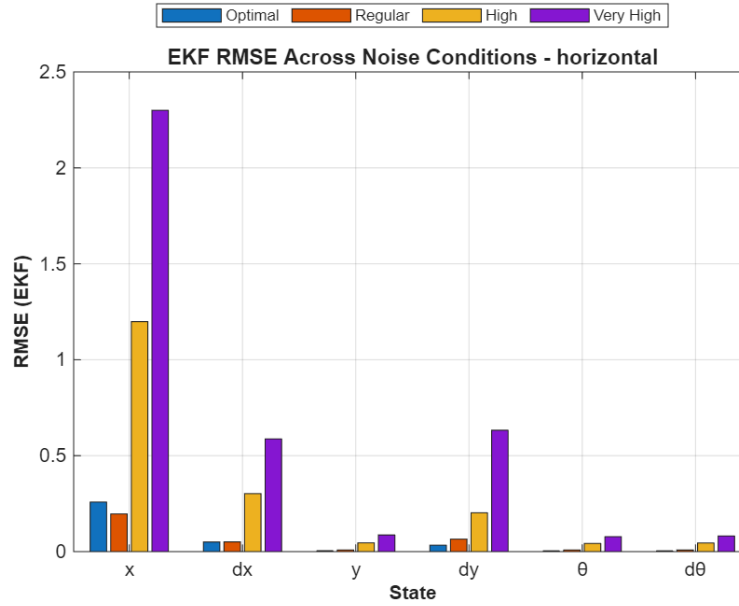


Figure 17: EKF RMSE across four noise levels for each state (horizontal recovery scenario). As expected,  $x$  is still different from the rest, for the same reasons as described in Figure 16 description. Maximum RMSE values have grown compared to the basic case because of the increased movement complexity.

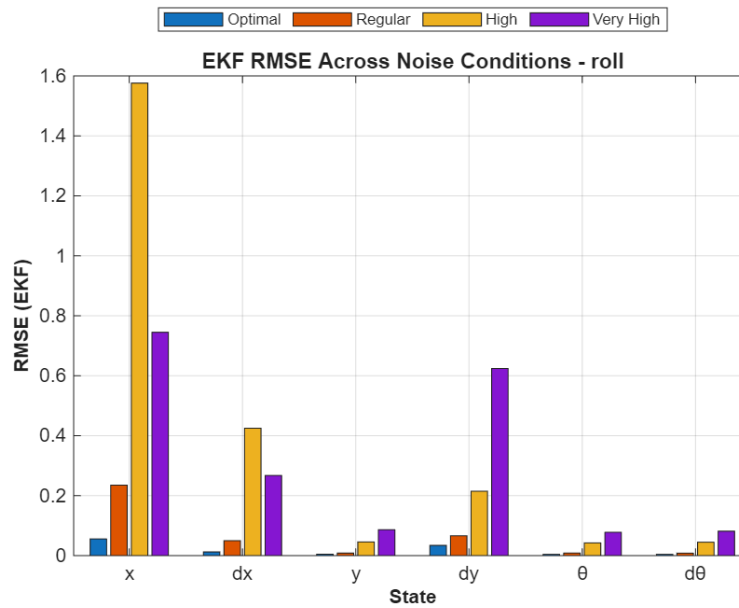


Figure 18: EKF RMSE across four noise levels for each state (roll scenario). Once again,  $x$  and its derivative display different RMSE progression when compared to the rest. This time, high variance leads to the highest RMSE values, even overtaking the very high variance.

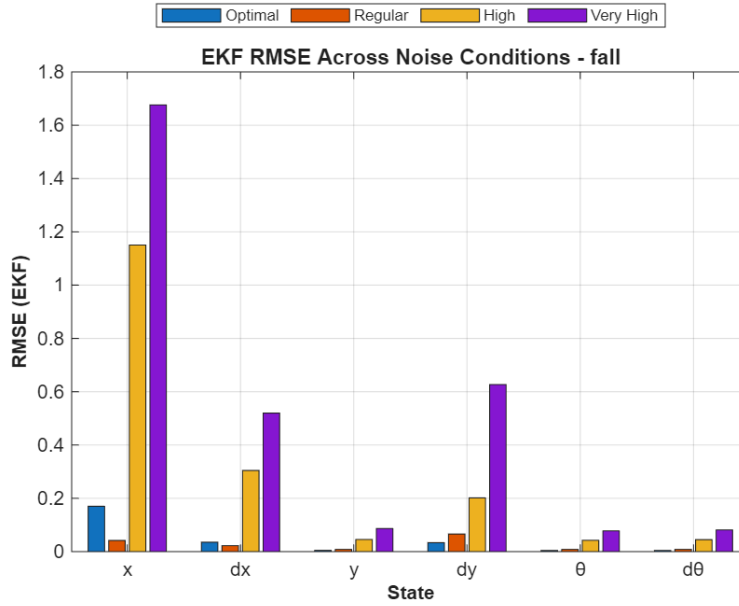


Figure 19: EKF RMSE across four noise levels for each state (fall recovery scenario). For a simple motion, same RMSE trend is seen as for the basic case (fig. 16), with similar RMSE values as well.

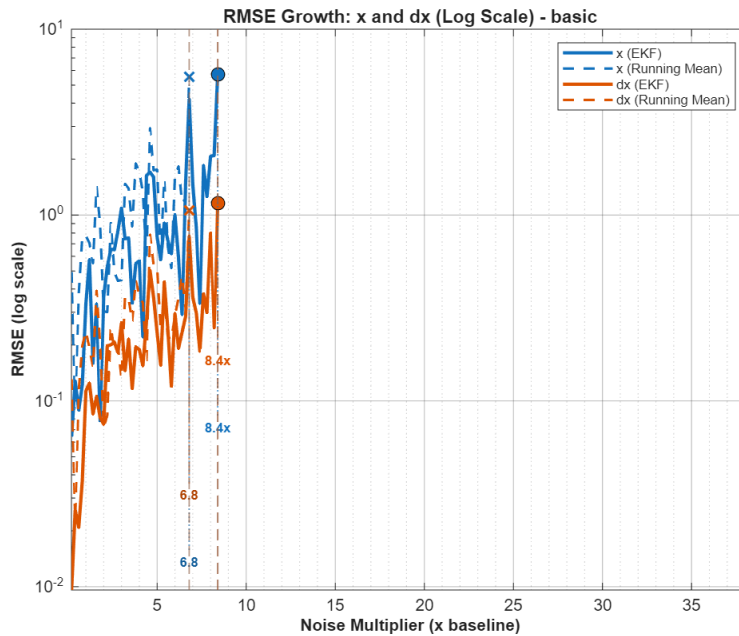


Figure 20: RMSE growth for  $x$  and  $\dot{x}$  under increasing noise (log scale, basic scenario). As discussed previously,  $x$  and  $\dot{x}$  are system parameters that have the biggest errors. In the simplest case, running mean is not so far from the EKF in terms of robustness.

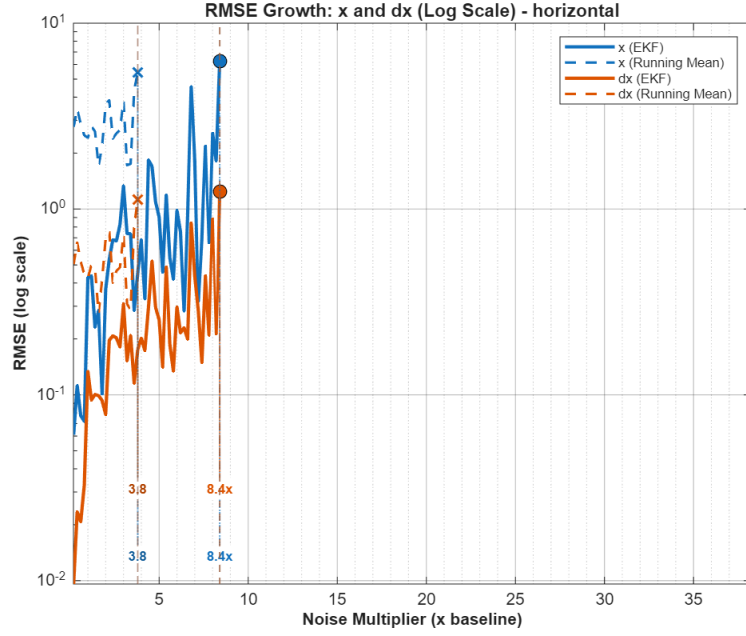


Figure 21: RMSE growth for  $x$  and  $\dot{x}$  under increasing noise (log scale, horizontal recovery scenario). Complex dynamic maneuvers are difficult for the running mean filter to track. Divergence of running mean happens significantly earlier compared to EKF.

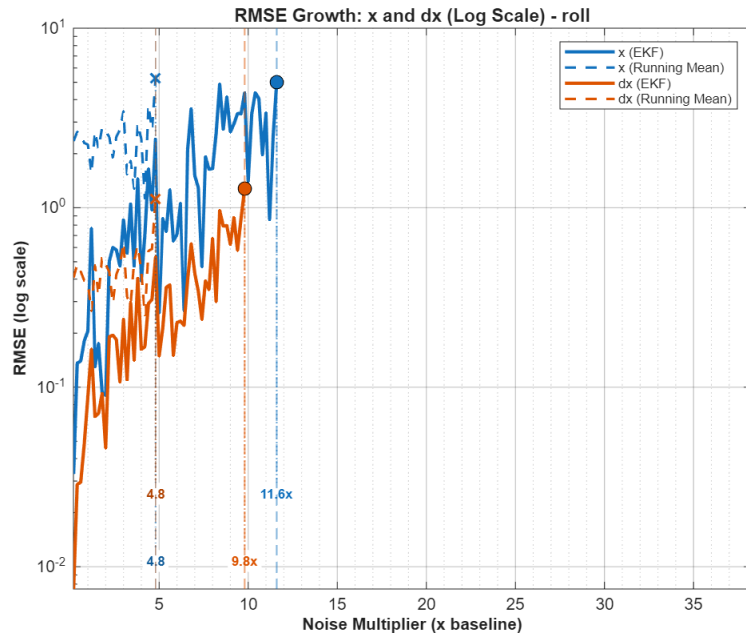


Figure 22: RMSE growth for  $x$  and  $\dot{x}$  under increasing noise (log scale, roll scenario). In this control-heavy scenario, the running mean diverges early once again. Interesting difference is early divergence of  $\dot{x}$ .

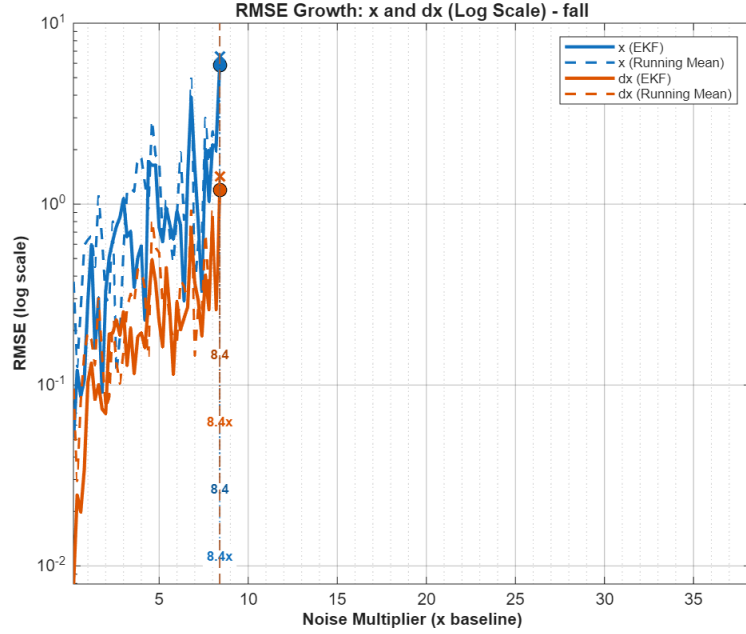


Figure 23: RMSE growth for  $x$  and  $\dot{x}$  under increasing noise (log scale, fall recovery scenario). As stated before, in simple simulations without rotation running mean is actually comparable in efficiency with the EKF.

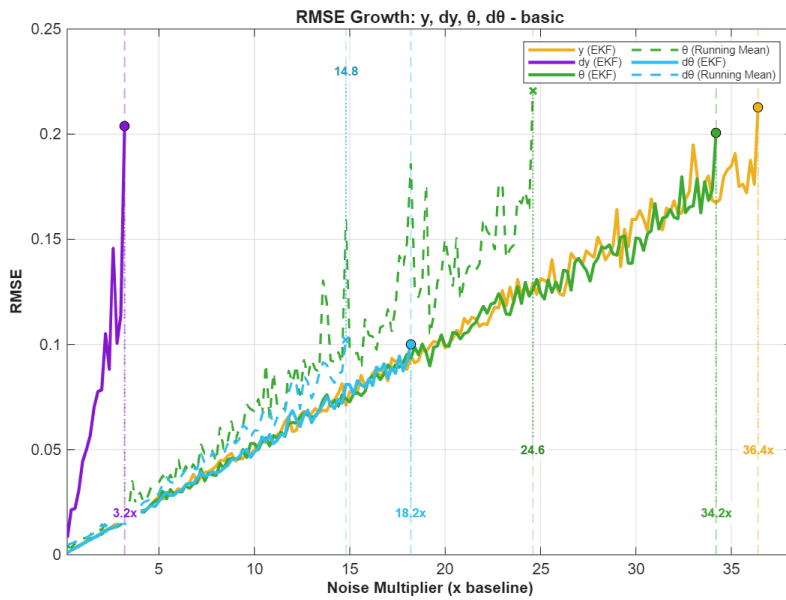


Figure 24: RMSE growth for  $y$ ,  $\dot{y}$ ,  $\theta$ , and  $\dot{\theta}$  under increasing noise (linear scale, basic scenario). Unlike the log scale of  $x$  and  $\dot{x}$ , other system parameters RMSE growth can be displayed on a linear scale. Measured parameters of the system have significantly higher variance multiplier required for divergence.

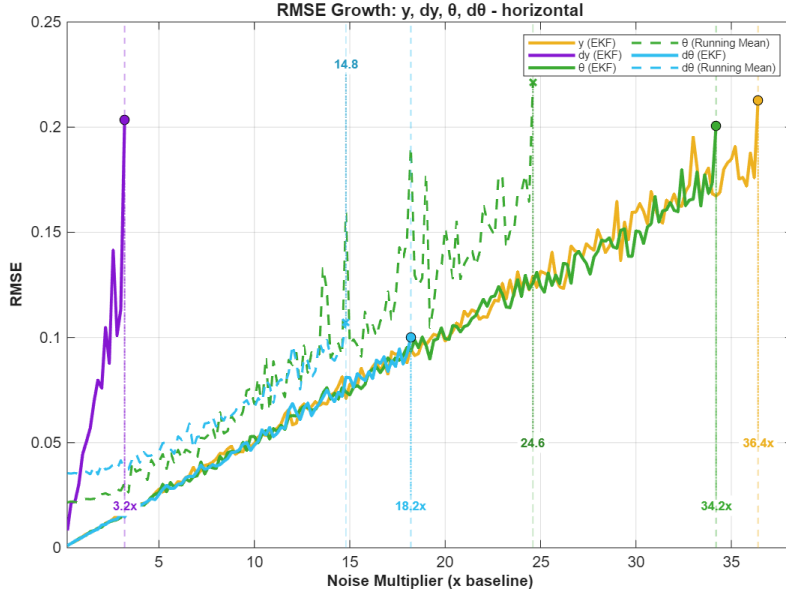


Figure 25: RMSE growth for  $y$ ,  $\dot{y}$ ,  $\theta$ , and  $\dot{\theta}$  under increasing noise (linear scale, horizontal recovery scenario). The only visible difference present is some slight running mean divergence multiplier (which shows how stable EKF is with different flight cases).

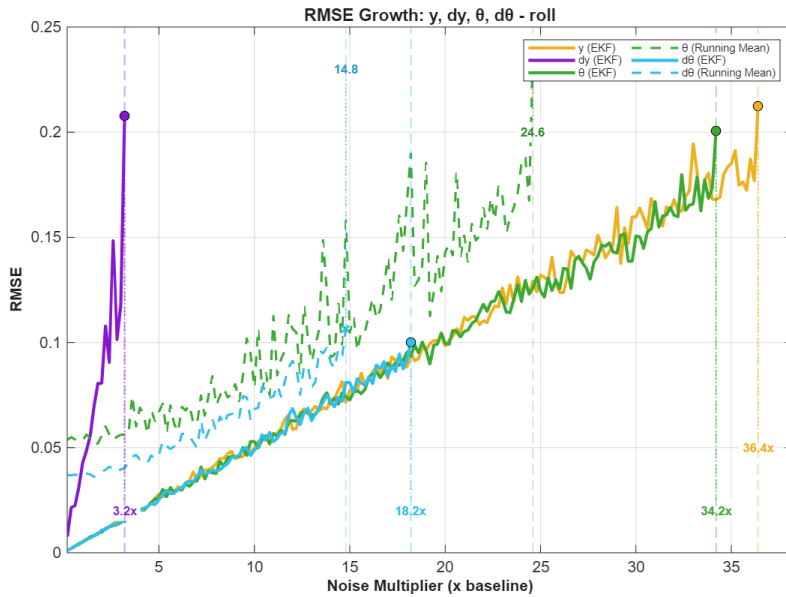


Figure 26: RMSE growth for  $y$ ,  $\dot{y}$ ,  $\theta$ , and  $\dot{\theta}$  under increasing noise (linear scale, roll scenario). Another case, another running mean multiplier change, EKF is stable as in the two previous examples (figs. 24, 25)

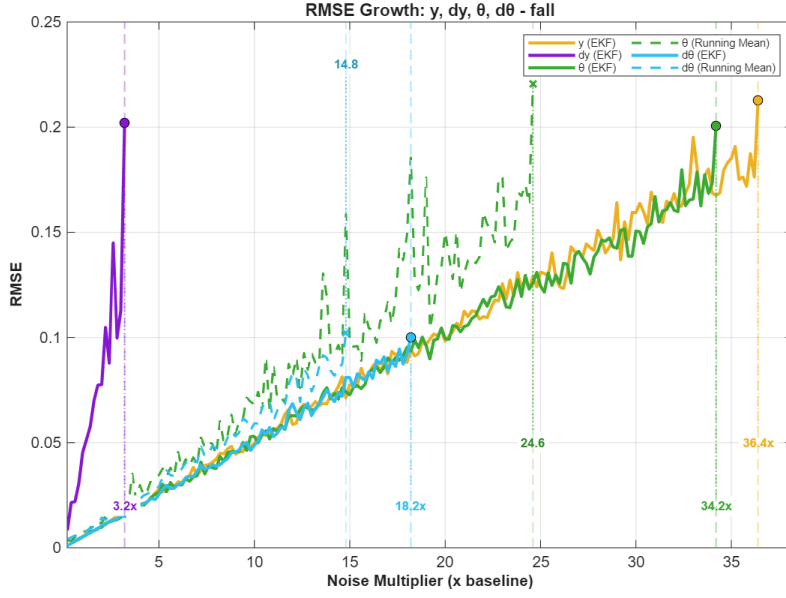


Figure 27: RMSE growth for  $y$ ,  $\dot{y}$ ,  $\theta$ , and  $\dot{\theta}$  under increasing noise (linear scale, fall recovery scenario). The last case definitely proves the point of EKF divergence multiplier stability for different flight conditions of the quadrotor system.

Table 1: RMSE Values for State Variables for the horizontal simulation scenario (figs. 4,8)

Variable	Kalman RMSE	Running Mean RMSE	Unfiltered RMSE
$x$	0.0417	0.6632	-
$\dot{x}$	0.0222	0.1866	-
$y$	0.0084	0.5453	0.0098
$\dot{y}$	0.0659	0.1902	-
$\theta$	0.0084	0.0100	0.0101
$\dot{\theta}$	0.0083	0.0095	0.0104

#### Analysis of Estimation Performance

The quantitative results presented in Table 1 demonstrate that the Extended Kalman Filter (EKF) significantly outperforms the running mean filter across all state

variables. This performance gap is most pronounced in the unobserved states—specifically horizontal position ( $x$ ), horizontal velocity ( $\dot{x}$ ), and vertical velocity ( $\dot{y}$ ). While the running mean filter achieves a Root Mean Square Error (RMSE) of 0.6632 m for the horizontal position, the EKF maintains an accuracy of 0.0417 m (fig. 12). This disparity arises because the running mean filter relies on a simplified kinematic propagation for unobserved states (Appendix B, lines 162–173), which lacks the corrective feedback mechanism found in the EKF’s state update equation (Eq. 23). The EKF’s superior handling of nonlinearities is evident in the "Roll" scenario (Figure 5). As the quadrotor undergoes a complete 360-degree rotation, the system dynamics become highly nonlinear due to the trigonometric coupling of the thrust vectors (Eq. 1-2). The running mean filter, which simply smooths the sensor output (Eq. 25) and integrates the result, fails to account for the rapid changes in orientation, leading to the unbounded error growth observed in Figure 13. Conversely, the EKF updates its Jacobian matrix  $F$  at every time step using the current state estimate (Appendix B, lines 108, 125-130), allowing it to accurately track the trajectory even during aggressive maneuvers.

### Robustness Testing Methodology

To evaluate the stability of the estimators under adverse conditions, a robustness analysis was conducted by systematically increasing the process and measurement noise levels. The testing procedure, implemented in robustness.m (Appendix C), applies a scalar multiplier to the baseline noise variances defined in the simulation (Appendix A, lines 112-113). The multiplier ranges from  $0.2\times$  to  $50\times$  the nominal values, effectively simulating sensor degradation and increasing environmental turbulence (Appendix C, lines 44-45).

To quantify the limits of stability, specific divergence thresholds were defined for each state variable. A filter is considered to have "diverged" when its Root Mean Square Error (RMSE) exceeds these pre-defined safety limits: 5.0 m for horizontal position ( $x$ ), 1.0 m/s for horizontal velocity ( $\dot{x}$ ), and 0.2 for both vertical position ( $y$ ) and vertical velocity ( $\dot{y}$ ) (Appendix C, line 70). Tighter constraints were applied to the rotational states, with thresholds of 0.2 rad for pitch angle ( $\theta$ ) and 0.1 rad/s for pitch rate ( $\dot{\theta}$ ), reflecting the critical importance of attitude estimation for stable flight (Appendix C, line 70). The robustness loop iterates through increasing noise multipliers until these specific thresholds are breached, recording the multiplier value at which failure occurs (Appendix C, line 85).

### Robustness Analysis Conclusions

The response to increasing noise reveals a fundamental difference in filter architecture. As illustrated in the logarithmic growth plots (Figures 20- 23), the error in the EKF estimates grows with the noise magnitude, maintaining stability even at high variance levels (figs. 16 - 19). In contrast, the running mean filter exhibits early divergence, particularly for the horizontal states ( $x$  and  $\dot{x}$ ). In the "Horizontal Recovery" scenario, the running mean's estimation of  $\dot{x}$  diverges significantly earlier than the EKF (Figure 21). This is attributed to the integration of noisy orientation data without covariance tracking; the EKF mitigates this by weighing the theoretical model against the noisy measurements via the Kalman Gain  $K$  (Eq. 20-22, Appendix B, line 142). The linear scale plots (Figures 24-27) further confirm that while observed states ( $y, \theta$ ) are relatively resilient in both filters due to direct sensor updates, the EKF provides a necessary layer of filtering that prevents high-frequency noise from corrupting the velocity estimates. Ultimately, the EKF proves to

be the robust solution required for the nonlinear dynamics of the planar quadrotor.

However, it is important to acknowledge that the filter was perfectly tuned in all the tested scenarios, implying that tuning is a key to robust performance.

Seed 47 was used for any random number generation in the report. All code can be accessed at <https://github.com/Arseni10Lk/Planar-Quadrotor>

## **Team Member Contributions**

### Formal Roles

Arseni Lysak - Lead

Tsimafei Iliusenka - System Modeling & Simulation Specialist

John Elvin Ndahiro - Presentation & Demonstration Specialist

Pablo Calderon Mateo - Technical Engineer

### Actual Tasks

Arseni Lysak:

- Task assignment, deadline setting and organization.
- Technical assistance with GitHub, Git, MATLAB, and LaTeX.
- Work review and quality assurance.
- Implementation of Real and Clean simulation code with error calculation (but not RMSE).
- Finalization of the EKF and Running Mean filter implementations.
- Adjustment and correction of critical mistakes in the plotting functions for simulation and robustness testing.

- Report writing and editing.

Tsimafei Iliusenka:

- Analytical solution to find Jacobian.
- Initial Extended Kalman filter design in code.
- Control inputs 2-4 design.
- Presentation template research.
- Presentation Design verification.
- **Always** delivered before the deadline.

John Elvin Ndahiro:

- Initial ReadMe file writing.
- Research to define typical physical parameters of a drone.
- Control input 1 design.
- Initial plotting functions for the simulation.
- Final plotting functions for Simulation and Robustness Testing.

Pablo Calderon Mateo:

- System definition in code.
- RMSE computation.
- Initial Robustness Testing System design.
- Base Noise Variance selection.
- Design of a running mean filter template.
- Presentation Design.

## Bibliography

Welch, Greg, and Gary Bishop. *An Introduction to the Kalman Filter*. Technical Report TR 95-041. Updated March 11, 2002. University of North Carolina at Chapel Hill, 2002.

### Planar \_ Quadrotor.m

```
1 clc;
2 clear;
3 close all;
4
5 rng(47);
6
7 %% DEFINE VARIABLES
8 m = 0.5;           % mass [kg]
9 r = 0.15;          % distance from center to rotors [m]
10 I = 0.005;         % moment of inertia [kg*m^2]
11 g = 9.81;          % gravity [m/s^2]
12 dt = 0.01;         % time step [s]
13 theta = 0;          % angle [rads]
14 u1 = 5;            % force [N]
15 u2 = 5;            % force [N]
16
17 % Structure definition
18 rotor_data.m = m;
19 rotor_data.r = r;
20 rotor_data.I = I;
21 rotor_data.g = g;
22 rotor_data.dt = dt;
23 rotor_data.theta = theta;
24 rotor_data.u1 = u1;
25 rotor_data.u2 = u2;
26
```

```

27 t_max = 10;           % simulation duration [s]

28

29 % A matrix - System dynamics

30 A = [0  1  0  0  0  0;
31 0  0  0  0  -cos(theta)*(u1+u2)/m  0;
32 0  0  0  1  0  0;
33 0  0  0  0  -sin(theta)*(u1+u2)/m  0;
34 0  0  0  0  0  1;
35 0  0  0  0  0  0];

36

37 % It describes the states, so let's say it is rotor data

38 rotor_data.A = A;

39

40 % C matrix - Measurements

41 C = [0  0  1  0  0  0;
42 0  0  0  0  1  0;
43 0  0  0  0  0  1];

44

45 rotor_data.C = C; % It says what we measure, so let's say it is rotor data

46 % (like what the sensors are)

47

48 %% STEP 4: DEFINE TIME VECTOR

49 time = 0:dt:t_max;

50

51 %% STEP 5: DEFINE CONTROL INPUTS

52 % Create CU1 and CU2 (basic case)

53 CU1 = u1 * 0.6 * (1 + 0.001*cos(2*time));

```

```
54 CU2 = u2 * 0.6 * (1 + 0.001*sin(2*time));  
55  
56 % Create CU3 and CU4 (horizontal flight recovery)  
57 CU3 = zeros(size(time));  
58 CU4 = zeros(size(time));  
59  
60 for t = 0:109 % roll up  
61 CU3(t + 1) = u1 * 0.81 * (1 + 0.001*cos(2 * 0.01 * t));  
62 CU4(t + 1) = u2 * 0.8 * (1 + 0.001*sin(2 * 0.01 * t));  
63 end  
64 for t = 110:219 % stop rotation  
65 CU3(t + 1) = u1 * 0.8 * (1 + 0.001*cos(2 * 0.01 * t));  
66 CU4(t + 1) = u2* 0.81 * (1 + 0.001*sin(2 * 0.01 * t));  
67 end  
68 for t = 220:length(time) % fly up  
69 CU3(t + 1) = u1 * 0.8 * (1 + 0.001*cos(2 * 0.01 * t));  
70 CU4(t + 1) = u2 * 0.8 * (1 + 0.001*sin(2 * 0.01 * t));  
71 end  
72  
73 % Create CU5 and CU6 (360 roll)  
74 CU5 = zeros(size(time));  
75 CU6 = zeros(size(time));  
76  
77 for t = 0:199 % initiate roll  
78 CU5(t + 1) = u1 * 0.808 * (1 + 0.001*cos(2 * 0.01 * t));  
79 CU6(t + 1) = u2 * 0.8 * (1 + 0.001*sin(2 * 0.01 * t));  
80 end
```

```

81 for t = 200:299 % let it roll
82 CU5(t + 1) = u1 * 0 * (1 + 0.001*cos(2 * 0.01 * t));
83 CU6(t + 1) = u2 * 0 * (1 + 0.001*sin(2 * 0.01 * t));
84 end
85 for t = 300:500 % stop rotation
86 CU5(t + 1) = u1 * 0 * (1 + 0.001*cos(2 * 0.01 * t));
87 CU6(t + 1) = u2 * 0.008 * (1 + 0.001*sin(2 * 0.01 * t));
88 end
89 for t = 501:length(time) % recover vertically
90 CU5(t + 1) = u1 * (1 + 0.001*cos(2 * 0.01 * t));
91 CU6(t + 1) = u2 * (1 + 0.001*sin(2 * 0.01 * t));
92 end
93
94 % Create CU7 and CU8 (straight fall recovery)
95 CU7 = u1 * 0.54 * (1 + 0.001*cos(2*time));
96 CU8 = u2 * 0.54 * (1 + 0.001*sin(2*time));
97
98 % Combine for sim
99 control_input.basic = [CU1; CU2]';
100 control_input.horizontal = [CU3; CU4]';
101 control_input.roll = [CU5; CU6]';
102 control_input.fall = [CU7; CU8]';
103
104
105 %% STEP 6: DEFINE NOISE AMPLITUDE & robustness testing
106
107 initial_state.basic = [0;0;1;0;0;0]; % basic case

```

```

108 initial_state.horizontal = [0;3;10;0;-pi/2;0]; % horizontal flight recovery
109 initial_state.roll = [0;0;50;5;0;0]; % roll
110 initial_state.fall = [0;-1;15;-3;-(pi/2-atan(3/1));0]; % straight fall recovery
111
112 noise_data.state_noise_amp = 0.003;
113 noise_data.output_noise_amp = 0.01;
114
115 %% STEP 7: SIMULATION
116
117 % Define the test case name here (e.g., 'fall', 'basic', 'roll', 'horizontal')
118 current_case = 'roll';
119
120 [states, output, error] = simulation_quadrotor(rotor_data, control_input.(current_case),
121
122 % Run Robustness
123 [rmse_mat, noise_mat, div_data, rmse_running] = robustness(rotor_data, control_input.(
124
125 % New functions with saving logic:
126 % Pass 'current_case' to save files with that specific name
127 % plot_robustness_separate_windows(rmse_mat, noise_mat, div_data, current_case);
128
129 plot_quadrotor_separate_windows(time, states, output, C, error, current_case);

```

## simulation\_quadrotor.m

```
1 function [state, output, errors] = simulation_quadrotor(rotor_data, control_input,
2   noise_data, time, x0)
3
4 % Three functions combined into one
5
6 % getting all the quadrotor characteristics
7 m = rotor_data.m;
8 r = rotor_data.r;
9 I = rotor_data.I;
10 g = rotor_data.g;
11 dt = rotor_data.dt;
12 C = rotor_data.C;
13 A = rotor_data.A;
14
15 if nargin == 4
16 x0 = zeros(1,6);
17 end
18
19 % Initialize output and states based on input parameters
20 output.clean = zeros(length(time), size(C, 1));
21 output.real = zeros(length(time), size(C, 1));
22 output.filtered = zeros(length(time), size(C, 1));
23 output.running = zeros(length(time), size(C, 1));%RUNNING
24
25 state.clean = zeros(length(time), size(A, 1));
26 state.real = zeros(length(time), size(A, 1));
27 state.estimate = zeros(length(time), size(A, 1));
```

```
27 state.running = zeros(length(time), size(A, 1));%RUNNING  
28  
29 % Simulate the system dynamics over the specified time  
30  
31 % Set initial state  
32 state.clean(1, :) = x0;  
33 state.real(1, :) = x0;  
34 state.estimate(1, :) = x0;  
35 state.running(1, :) = x0;%RUNNING  
36  
37 output.clean(1, :) = C*state.clean(1, :)';  
38 output.real(1, :) = output.clean(1, :);  
39 output.filtered(1, :) = output.clean(1, :);  
40 output.running(1, :) = output.clean(1, :);%RUNNING  
41  
42 % Filter data  
43  
44 P = eye(6); % Initial Uncertainty  
45 % Q: Process Noise Covariance (Trust in Physics)  
46 % We use a small value to allow the model to drive the smoothness  
47 Q = eye(6) * (0.003^2);  
48 % R: Measurement Noise Covariance (Trust in Sensors)  
49 % We set this higher than actual noise to filter out the jitters  
50 R = eye(3) * (0.01^2);  
51  
52 % Running  
53 window_size = 10; % You can adjust this window size
```

```

54
55 for t = 2:length(time)
56
57 %% Perfect simulation
58
59 % update theta
60 theta_clean = state.clean(t - 1, 5);
61
62 % Update states based on linear dynamics, this works for everything
63 % except dx and dy
64 delta_x_clean(1) = state.clean(t - 1, 2)*dt;
65 delta_x_clean(3) = state.clean(t - 1, 4)*dt;
66 delta_x_clean(5) = state.clean(t - 1, 6)*dt;
67 delta_x_clean(6) = (r / I * control_input(t, 1) - r / I * control_input(t, 2)) * dt;
68
69 % Now, non-linear part
70 delta_x_clean(2) = (-sin(theta_clean)*(control_input(t, 1)+control_input(t, 2))/m) * dt;
71 delta_x_clean(4) = (cos(theta_clean)*(control_input(t, 1)+control_input(t, 2))/m - g) * dt;
72
73
74 % Lastly, updating states
75 state.clean(t, :) = state.clean(t-1, :) + delta_x_clean(:)';
76 output.clean(t, :) = (C * state.clean(t, :))';
77
78 %% Real-world simulation
79
80 % update theta

```

```

81 theta_real = state.real(t - 1, 5);

82

83 % Update states based on linear dynamics, this works for everything

84 % except dx and dy

85 delta_x_real(1) = state.real(t - 1, 2)*dt;

86 delta_x_real(3) = state.real(t - 1, 4)*dt;

87 delta_x_real(5) = state.real(t - 1, 6)*dt;

88 delta_x_real(6) = (r / I * control_input(t, 1) - r / I * control_input(t, 2)) * dt;

89

90 % Now, non-linear part

91 delta_x_real(2) = (-sin(theta_real)*(control_input(t, 1)+control_input(t, 2))/m) * dt;

92 delta_x_real(4) = (cos(theta_real)*(control_input(t, 1)+control_input(t, 2))/m - g) * dt;

93

94 % getting all the noise characteristics

95 state_noise = noise_data.state_noise_amp * randn(1, size(A, 1));

96 output_noise = noise_data.output_noise_amp * randn(1, size(C, 1));

97

98 state.real(t, :) = state.real(t - 1, :) + delta_x_real(:)' + state_noise;

99 output.real(t, :) = (C*state.real(t, :)')' + output_noise;

100

101 %% Filter

102 % Filter uses perfect physics and sensor measurements, but we do not pass

103 % real state to it.

104

105 % PREDICTION STEP

106

107 % update theta

```

```

108 theta_estimate = state.estimate(t - 1, 5);

109

110 % Update states based on linear dynamics, this works for everything

111 % except dx and dy

112 delta_x_estimate(1) = state.estimate(t - 1, 2)*dt;

113 delta_x_estimate(3) = state.estimate(t - 1, 4)*dt;

114 delta_x_estimate(5) = state.estimate(t - 1, 6)*dt;

115 delta_x_estimate(6) = (r / I * control_input(t, 1) - r / I * control_input(t, 2)) * dt;

116

117 % Now, non-linear part

118 delta_x_estimate(2) = (-sin(theta_estimate)*(control_input(t, 1)+control_input(t, 2))/m) *

119 delta_x_estimate(4) = (cos(theta_estimate)*(control_input(t, 1)+control_input(t, 2))/m - g)

120 * dt;

121 state.estimate(t, :) = state.estimate(t - 1, :) + delta_x_estimate(:)';

122

123 % Predict covariance

124

125 F = eye(6) + dt * [0 1 0 0 0 0;

126 0 0 0 0 -cos(theta_estimate)*(control_input(t, 1)+control_input(t, 2))/m 0;

127 0 0 0 1 0 0;

128 0 0 0 0 -sin(theta_estimate)*(control_input(t, 1)+control_input(t, 2))/m 0;

129 0 0 0 0 0 1;

130 0 0 0 0 0 0];

131

132 P_prediction = F * P * F' + Q;

```

```

133
134 % CORRECTION STEP
135
136 % 1. Calculate Measurement Residual
137 measurement_residual = output.real(t, :)' - C * state.estimate(t, :)';
138 measurement_residual(2) = mod(measurement_residual(2) + pi, 2*pi) - pi;
139
140 % 2. Calculate Kalman Gain
141 S = C * P_prediction * C' + R;
142 K = P_prediction * C' / S;
143
144 % 3. Update State Estimate
145 state.estimate(t, :) = state.estimate(t, :) + (K * measurement_residual)';
146 output.filtered(t, :) = C * state.estimate(t, :)';
147
148 % 4. Update Covariance
149 P = (eye(6) - K * C) * P_prediction;
150
151
152 % RUNNING
153 % Determine the start of the window
154 window_start = max(1, t - window_size);
155
156 % Average the noisy measurements ('real' outputs) over the window
157 output.running(t, :) = mean(output.real(window_start:t, :), 1);
158
159 % update theta

```

```

160 theta_running = output.running(t, 2);

161

162 state.running(t, 3) = output.running(t, 1); % Overwrite y (State 3)

163 state.running(t, 5) = output.running(t, 2); % Overwrite theta (State 5)

164 state.running(t, 6) = output.running(t, 3); % Overwrite theta_dot (State 6)

165

166 % For the states, we apply the same averaging to the noisy running states

167 % Update states based on linear dynamics, this works for everything

168 % except dx and dy

169 delta_x_running(1) = state.running(t-1, 2) * dt;

170

171 % Now, non-linear part

172 delta_x_running(2) = (-sin(theta_running)*(control_input(t, 1)+control_input(t, 2))/m) * dt;

173 delta_x_running(4) = (cos(theta_running)*(control_input(t, 1)+control_input(t, 2))/m - g) *

174 dt;

175 state.running(t, [1 2 4]) = state.running(t - 1, [1 2 4]) + delta_x_running([1 2 4]);

176

177 end

178

179

180 %RUNNING

181 errors.output_clean_VS_running_total = output.running - output.clean;

182 errors.states_real_VS_running = state.real - state.running;

183

184 errors.output_clean_VS_real_total = output.real - output.clean;

185 errors.output_clean_VS_filtered_total = output.filtered - output.clean;

```

```
186 errors.output_real_VS_filtered_total = output.filtered - output.real;  
187  
188 errors.states_clean_VS_real_total = state.real - state.clean;  
189 errors.states_real_VS_estimate = state.real - state.estimate;  
190 errors.state_real_VS_output_real = output.real - state.real(:, [3, 5, 6]);  
191 errors.state_real_VS_output_filtered = output.filtered - state.real(:, [3, 5, 6]);  
192  
193 % Calculate the Mean Squared Error for each column (state variable)  
194 num_states = size(errors.states_real_VS_estimate, 2);  
195 rmse_values = zeros(1, num_states);  
196 rmse_running = zeros(1, num_states);  
197  
198  
199 for i = 1:num_states  
200 % RMSE = sqrt(mean(error^2))  
201 rmse_values(i) = sqrt(mean(errors.states_real_VS_estimate(:, i).^2));  
202 %RUNNING  
203 rmse_running(i) = sqrt(mean(errors.states_real_VS_running(:, i).^2));  
204 end  
205  
206 rmse_unfiltered = zeros(1, 3);  
207  
208 for i = 1:3  
209 rmse_unfiltered(i) = sqrt(mean(errors.state_real_VS_output_real(:, i).^2));  
210 end  
211  
212 % Store the RMSE values in the errors structure
```

```

213
214 % state variables are typically: [x, dx, y, dy, theta, dtheta]
215 errors.rmse_states = rmse_values;
216 %RUNNING
217 errors.rmse_running = rmse_running;
218
219 errors.rmse_unfiltered = rmse_unfiltered;
220 end
221

```

### robustness.m

```

1 function [rmse_matrix, noise_matrix, divergence_data, rmse_matrix_running] = robustness(
2     rotor_data, control_input, time, initial_state, noise_data_base)
3 % ROBUSTNESS - Run robustness tests and return data for plotting
4 % Returns: rmse_matrix (Kalman), noise_matrix, divergence_data, rmse_matrix_running (Running
5 )
6
7 % Define 4 noise cases (Cases 1-4)
8 noise_cases = [
9 0.0015, 0.01; % Case 1: Optimal
10 0.003, 0.02; % Case 2: Regular
11 0.015, 0.1; % Case 3: High noise
12 0.03, 0.2 % Case 4: Very high noise
13 ];
14

```

```
15 num_cases = size(noise_cases, 1);
16 rmse_matrix = zeros(num_cases, 6);
17 rmse_matrix_running = zeros(num_cases, 6); % NEW: Store running filter RMSE
18 noise_matrix = noise_cases;
19
20 % Run simulations for Cases 1-4
21 for case_num = 1:num_cases
22 noise_data.state_noise_amp = noise_cases(case_num, 1);
23 noise_data.output_noise_amp = noise_cases(case_num, 2);
24
25 [~, ~, errors] = simulation_quadrotor(rotor_data, control_input, noise_data, time,
26 initial_state);
27
28 rmse_matrix(case_num, :) = errors.rmse_states;
29 rmse_matrix_running(case_num, :) = errors.rmse_running; % NEW
30
31 fprintf('Case %d RMSE (Kalman): ', case_num);
32 fprintf('%.4f ', errors.rmse_states);
33 fprintf('\n');
34 end
35
36 % Run divergence analysis
37 divergence_data = find_divergence_individual_states(rotor_data, control_input, time,
38 initial_state, noise_data_base);
39
40 fprintf('\n==== Analysis Complete ===\n');
```

```

40

41 %% ====== HELPER FUNCTION - TRACKS INDIVIDUAL STATE DIVERGENCE ======
42 function div_data = find_divergence_individual_states(rotor_data, control_input, time,
43 initial_state, noise_data_base)
44 base_noise = [noise_data_base.state_noise_amp, noise_data_base.output_noise_amp]; % Base
45 % noise levels
46 max_multiplier = 50;
47 multiplier = 0.2;
48
49 div_data.multipliers = [];
50
51 % State names
52 state_names = {'x', 'dx', 'y', 'dy', 'theta', 'dtheta'};
53 display_names = {'x', 'dx', 'y', 'dy', 'θ', 'dθ'};
54 div_data.state_names = state_names;
55 div_data.display_names = display_names;
56
57 % Initialize divergence tracking for BOTH filters
58 for i = 1:6
59 % Kalman Tracking
60 div_data(['div_point_' state_names{i}]) = 0;
61 div_data(['actually_diverged_' state_names{i}]) = false;
62 div_data(['threshold_' state_names{i}]) = 0;
63
64 % NEW: Running Filter Tracking

```

```

65 div_data.(['div_point_running_' state_names{i}]) = 0;
66 div_data.(['actually_diverged_running_' state_names{i}]) = false;
67 end
68
69 % Thresholds (Shared between filters)
70 thresholds = [5.0, 1.0, 0.2, 0.2, 0.2, 0.1];
71 for i = 1:6
72 div_data.(['threshold_' state_names{i}]) = thresholds(i);
73 end
74
75 fprintf('\n--- Starting Dual-Filter Divergence Analysis ---\n');
76
77 iteration = 0;
78 while multiplier <= max_multiplier
79 iteration = iteration + 1;
80 noise_data.state_noise_amp = base_noise(1) * multiplier;
81 noise_data.output_noise_amp = base_noise(2) * multiplier;
82
83 [~, ~, errors] = simulation_quadrotor(rotor_data, control_input, noise_data, time,
84 initial_state);
85
85 div_data.multipliers(end+1) = multiplier;
86 div_data.rmse_values(end+1, :) = errors.rmse_states;
87 div_data.rmse_values_running(end+1, :) = errors.rmse_running; % NEW
88
89 % Check EACH STATE for divergence (Kalman & Running)
90 for state_idx = 1:6

```

```

91 threshold = thresholds(state_idx);

92 s_name = state_names{state_idx};

93

94 % 1. Check Kalman

95 if errors.rmse_states(state_idx) > threshold

96 if ~div_data(['actually_diverged_' s_name])

97 div_data(['actually_diverged_' s_name]) = true;

98 div_data(['div_point_' s_name]) = multiplier;

99 fprintf(' [Kalman] %s diverged at %.1fx\n', display_names{state_idx}, multiplier);

100 end

101 end

102

103 % 2. Check Running (NEW)

104 if errors.rmse_running(state_idx) > threshold

105 if ~div_data(['actually_diverged_running_' s_name])

106 div_data(['actually_diverged_running_' s_name]) = true;

107 div_data(['div_point_running_' s_name]) = multiplier;

108 fprintf(' [Running] %s diverged at %.1fx\n', display_names{state_idx}, multiplier);

109 end

110 end

111 end

112

113 % Progress

114 if mod(iteration, 10) == 0

115 fprintf(' Progress: %.1f/%.1f\n', multiplier, max_multiplier);

116 end

117

```

```
118 % Early exit: Only if BOTH filters have failed on ALL states
119 all_diverged = true;
120 for state_idx = 1:6
121 s_name = state_names{state_idx};
122 if ~div_data.(['actually_diverged_' s_name]) || ~div_data.(['actually_diverged_running_'
123 s_name])
124 all_diverged = false;
125 break;
126 end
127
128 if all_diverged
129 fprintf(' All states in both filters diverged. Stopping.\n');
130 break;
131 end
132
133 multiplier = multiplier + 0.2;
134 end
135
136 % Cleanup: Set stable states to max_tested
137 max_tested = max(div_data.multipliers);
138 div_data.max_multiplier_tested = max_tested;
139
140 for state_idx = 1:6
141 s_name = state_names{state_idx};
142 if ~div_data.(['actually_diverged_' s_name])
143 div_data.(['div_point_' s_name]) = max_tested;
```

```
144 end  
145 if ~div_data.(['actually_diverged_running_' s_name])  
146 div_data.(['div_point_running_' s_name]) = max_tested;  
147 end  
148 end  
149 end  
150
```